Relation between the PCB Near Field and the Common Mode Coupling from the PCB to Cables

Christian Poschalko #1 and Siegfried Selberherr *2

#Diesel & Gasoline Systems, Robert Bosch AG
Geiereckstrasse 6, A-1110 Vienna, AUSTRIA
[1]christian.poschalko@at.bosch.com

*Institute for Microelectronics, Technische Universitaet Wien
Gusshausstrasse 27-29/360, A-1040 Vienna, AUSTRIA
[2]Selberherr@TUWien.ac.at

***Abstract*— The common mode coupling from PCB sources to cables is one of the most significant emission mechanisms. We obtain a design expression for the common mode coupling inductance of a PCB trace inside a cavity from the cavity field, which is excited by this trace. This reveals a general relation between the coupling of PCB sources to a cavity and the common mode coupling to cables. In a second step we show that the coupling of a PCB to a parallel plane cavity can be obtained from the PCB near field.**

I. Introduction

The magnetic flux lines wrapping around the ground plane of a PCB cause a voltage between wires which are connected at the PCB [1]. Fig. 1 shows the magnetic flux and the associated common mode voltage U_{cm}, which drives a current on the cables, connected to the PCB. This current causes common mode emission from the cables. Near field scanning

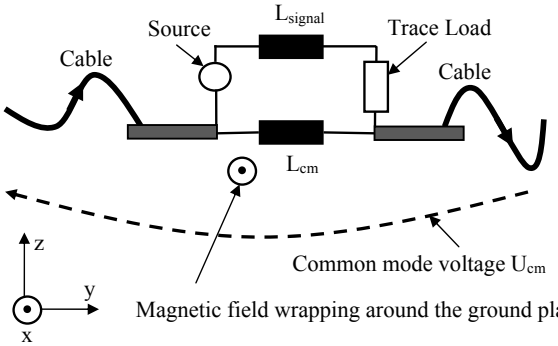

Fig. 1. Model illustrating the physics of the current driven common mode mechanism as described in [1].

over a PCB is a state of the art method to investigate the EMC performance of PCBs experimentally [2], [3]. Usually the magnetic field vector components $|H_x|$, $|H_y|$ and $H_{mag} = \sqrt{|H_x|^2 + |H_y|^2}$ are scanned versus frequency as depicted in Fig. 2. Increased field value areas on the PCB are observed as potential electromagnetic emission sources. However, an explicit relation between the scanned near field and the common mode voltage U_{cm} is missing. Since the common mode coupling of a PCB trace to cables depends

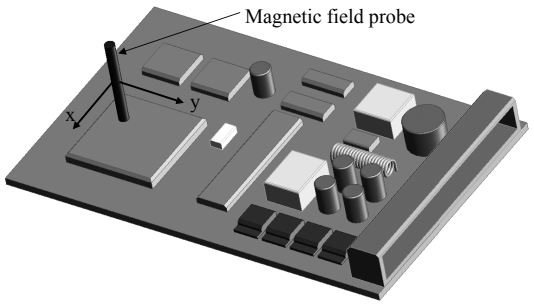

Fig. 2. Scanning the magnetic field above the PCB with a magnetic field probe.

on the trace geometry and the trace position on the PCB and not only on the trace current magnitude, critical areas on the PCB cannot generally be assigned to areas with increased near field magnitudes. In Section II we obtain the common mode inductance L_{cm} for a PCB trace inside a parallel plane cavity from the cavity model of [4]. We verify this L_{cm} with measurements and a comparison with the common mode inductance formulation for parallel planes of [5]. This provides the relation between the coupling of PCB traces to the cavity and the common mode inductance of these traces. In Section III we describe a method to obtain the PCB coupling to a cavity from the magnetic near field above the PCB. Thus, we achieve a quantitative relationship between the PCB near field and the common mode coupling from sources on the PCB to cables.

II. Derivation of the common mode inductance of a PCB trace inside a cavity

The differential mode current on the trace I_{dm} and common mode inductance L_{cm} in Fig. 1 determine the common mode voltage

$$U_{cm} = j\omega L_{cm} I_{dm}. \tag{1}$$

For a trace in the symmetry line (x=L/2) of the ground plane (Trace a in Fig. 3) the common mode inductance is

$$L_{cm} = \frac{4\mu d l_t}{\pi^2 L} \tag{2}$$

according to [5]. The trace length is l_t.

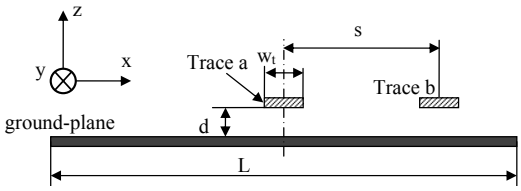

Fig. 3. Trace a in the symmetry line of the ground plane and Trace b located at a distance s from that symmetry line.

The trace inductance for a trace located at a distance s from the ground plane symmetry line (Trace b in Figure 3) is

$$L_{cm} = \frac{\mu l_t}{2\pi} \ln \left| 2\frac{s+jd}{L} + \sqrt{4\left(\frac{s+jd}{L}\right)^2 - 1} \right| \quad (3)$$

according to [6]. A trace in the symmetry line of the ground plane (s=0) [6] reduces (3) to

$$L_{cm} = \frac{\mu d l_t}{\pi L}. \quad (4)$$

The equations (2) and (4) have been obtained for a narrow trace ($w_t \ll L$) above the PCB ground plane and without a metallic cover plane. For a parallel plane structure ($w_t = L$, trace width = ground plane width) the common mode inductance is

$$L_{cm\_p} = \frac{h\mu l_t}{2L} \quad (5)$$

according to [5], where h is the plane separation distance.

A μ-TEM cell measurement with a hybrid coupler was carried out by [7] to obtain the coupling from heat sinks to cables and by [8] to obtain the magnetic moment for the coupling of a trace to cables. This measurement configuration is shown in Fig. 4. The coordinate system definition is consistent with those in Fig. 1 and Fig. 3. The magnetic field coupling moment

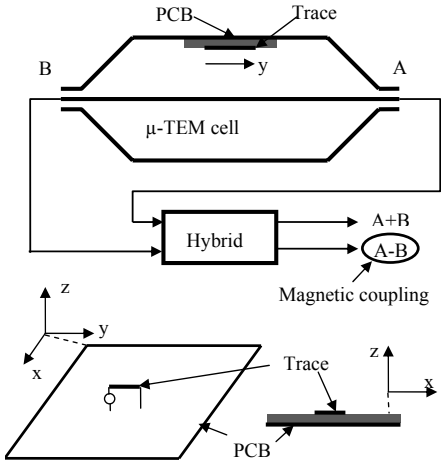

Fig. 4. Measurement configuration of [8] to obtain the magnetic coupling moment of a trace or an IC.

is obtained from the $A-B$ output of the hybrid coupler by [8]. To obtain the magnetic coupling of a trace to the cavity between two parallel rectangular planes, the model depicted in Fig. 5 is utilized. The voltages

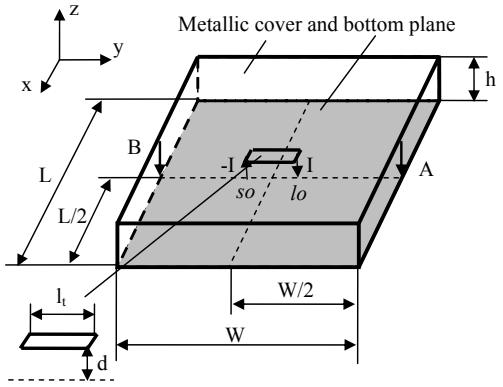

Fig. 5. Model for the derivation of the coupling inductance from a trace to the cavity.

$$U_i(x_i, y_i) = \sum_{j=1}^{n_{port}} (Z_{ij}(x_i, y_i, x_j, y_j) I_j(x_j, y_j)) \quad (6)$$

on ports, defined between the cover and the bottom plane of the rectangular cavity, are related to the port currents $I_j(x_j, y_j)$ by the impedance matrix. The coordinates of Port i and Port j are (x_i, y_i) and (x_j, y_j) respectively. Indexes i and j run from $1 \ldots n_{port}$, where n_{port} the number of ports. According to [9], the impedance matrix elements are

$$Z_{ij} = \frac{j\omega\mu h}{LW} \sum_{m=0}^{\infty} \sum_{n=0}^{\infty} \frac{L_m L_n N_i N_j}{k_m^2 + k_n^2 - (2\pi/\lambda)^2}, \quad (7)$$

with

$$N_i = \cos(k_m x_i) \cos(k_n y_i) \,\mathrm{si}\left(\frac{k_m w_{xi}}{2}\right) \mathrm{si}\left(\frac{k_n w_{yi}}{2}\right), \quad (8)$$

$$N_j = \cos(k_m x_j) \cos(k_n y_j) \,\mathrm{si}\left(\frac{k_m w_{xj}}{2}\right) \mathrm{si}\left(\frac{k_n w_{yj}}{2}\right), \quad (9)$$

$$k_m = \frac{m\pi}{L_e},\ k_n = \frac{n\pi}{W_e}, \quad (10)$$

and

$$\mathrm{si}(x) = \frac{\sin(x)}{x}. \quad (11)$$

L_m are one for $m = 0$ and two for nonzero m. L_n are one for $n = 0$ and two for nonzero n. The port dimensions for the rectangular ports i and j are (w_{xi}, w_{yi}) and (w_{xj}, w_{yj}) respectively and λ is the wavelength. The coupling from a trace, like in Fig. 5, to the cavity field is considered with two ports in (6) according to [4]. One port at the source position *so* of the trace and a second port at the load position *lo* of the trace. For the introduction of the trace to (6), the trace currents have to be weighted by the trace to cavity coupling factor d/h. Since we need only mutual impedances to express the coupling from the trace to the cavity ports A and B in Fig. 5, we neglect the si() terms in (8) and (9). With the ports and the trace in Fig. 5 the voltage difference of Port A and Port B becomes

$$U_{AB} = -\frac{j\omega\mu h I}{LW}\frac{d}{h} \sum_{m=0}^{\infty} \sum_{n=0}^{\infty} \frac{L_m L_n K_t (1-(-1)^n) \cos^2(\frac{m\pi}{2})}{(\frac{m\pi}{L})^2 + (\frac{n\pi}{W})^2 - (\frac{2\pi}{\lambda})^2}, \quad (12)$$

with

$$K_t = \cos\left(\frac{n\pi}{W}\left(\frac{W}{2}+\frac{l_t}{2}\right)\right) - \cos\left(\frac{n\pi}{W}\left(\frac{W}{2}-\frac{l_t}{2}\right)\right) \tag{13}$$

According to the factor $(1-(-1)^n)$ terms with even n vanish. The nominator term $(2\pi/\lambda)$ may be neglected for low frequencies $W \ll \lambda$. With this simplification, (12) becomes

$$U_{AB} = j\omega M_c I = \frac{4j\omega\mu dI}{LW} \sum_{m=0}^{\infty}\sum_{n=0}^{\infty} \frac{L_m \sin\left(\frac{n\pi}{2}\right)\sin\left(\frac{n\pi l_t}{2W}\right)\left(1-(-1)^n\right)}{(\frac{2m\pi}{L})^2+(\frac{n\pi}{W})^2}$$
$$= \frac{8j\omega\mu dI}{LW}\sum_{m=0}^{\infty}\sum_{n=0}^{\infty}\frac{L_m(-1)^n\sin\left(\frac{(2n+1)\pi l_t}{2W}\right)}{(\frac{2m\pi}{L})^2+(\frac{(2n+1)\pi}{W})^2}. \tag{14}$$

The coupling inductance of the trace inside the cavity is

$$M_c = \frac{8\mu d}{LW}\sum_{n=0}^{\infty}\left[(-1)^n\sin\left(\frac{(2n+1)\pi l_t}{2W}\right) \left\{\frac{1}{\frac{(2n+1)\pi}{W})^2}+\sum_{m=1}^{\infty}\frac{2}{(\frac{2m\pi}{L})^2+(\frac{(2n+1)\pi}{W})^2}\right\}\right]. \tag{15}$$

With

$$\sum_{m=1}^{\infty}\frac{1}{a^2+m^2} = \frac{1}{2}\frac{\pi\coth(a\pi)a-1}{a^2}, \tag{16}$$

(15) is simplified to

$$M_c = \frac{4\mu d}{\pi} \sum_{n=0}^{\infty}\left[(-1)^n\sin\left(\frac{(2n+1)\pi l_t}{2W}\right)\frac{\coth\left(\frac{(2n+1)\pi L}{2W}\right)}{2n+1}\right]. \tag{17}$$

For small traces $l_t \ll W$ the function described by the fourier series in (17) is approximated by the first term of its Taylor series, developed around $l_t = 0$ and (17) becomes

$$M_c = \frac{2\mu d l_t}{W}\sum_{n=0}^{\infty}\left[(-1)^n\coth\left(\frac{(2n+1)\pi L}{2W}\right)\right]. \tag{18}$$

With

$$\sum_{n=0}^{\infty}\left[(-1)^n\coth\left(\frac{(2n+1)\pi L}{2W}\right)\right] \approx \frac{\pi}{4}\coth\left(\frac{L\pi}{2W}\right) \tag{19}$$

and

$$\coth(x) \approx \frac{1}{x} \quad \forall \quad |x|<1, \tag{20}$$

the coupling inductance for $L < (2/\pi)W \approx 0.6W$ becomes

$$M_c = \frac{\mu d l_t}{L}. \tag{21}$$

The common mode inductance is associated with the flux wrapping around only one of the two planes. Thus, the coupling inductance has to be divided by a factor of two to obtain the common mode inductance [5]. Therefore, the common mode inductance of a trace inside a parallel plane cavity is

$$\boxed{L_{cm\_p} = \frac{\mu d l_t}{2L}}. \tag{22}$$

Note that (22) becomes exactly (5) of [5], when the trace height above the ground plane is identical to the plane separation distance h. Equation (5) has been verified experimentally by [5]. We have carried out VNA (vector network analyzer) measurements with the setup in Fig. 6 to verify (22). The dimensions of the test setup are $W = 120mm$, $L = 50mm$, $l_t = 10mm$, $d = 1mm$, $h = 10mm$, $w_t = 2mm$, and $l_l = 500mm$. One measurement is carried out with a cover plane and a second measurement without the cover plane.

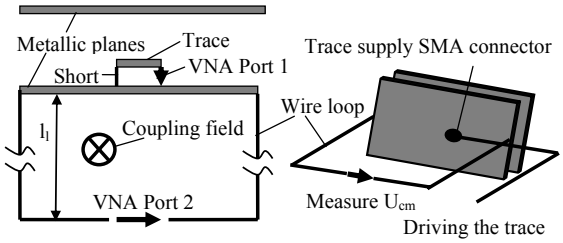

Fig. 6. Measurement of the common mode inductance. A trace loop above a copper plane is connected to one port of the VNA. The trace is terminated with 0 Ohm to the ground copper plane. A wire loop is soldered to both ends of the copper plane and a SMA connector in this loop is connected to the second VNA port for the measurement of the induced common mode loop voltage.

Fig. 7 shows good agreement of the measured common mode inductances to the analytical results from (4) of 0.08nH for the configuration without a cover plane and to the result from (22) of 0.12nH for the configuration with a cover plane. This provides evidence that the current driven common mode coupling mechanism of a trace inside a parallel-plane cavity to cables is described sufficiently with the cavity model. The cavity model describes not only the common mode mechanism for a tiny trace in the symmetry line of the cavity, but also the common mode coupling for arbitrary traces inside the cavity.

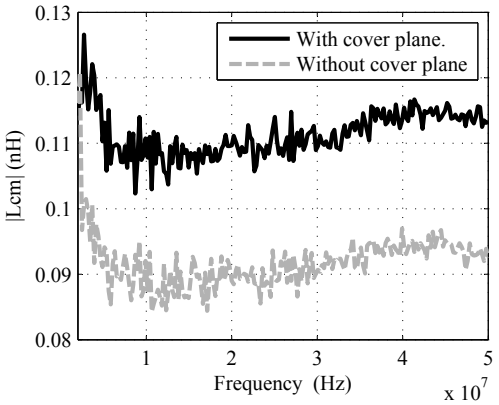

Fig. 7. Measured results for the common mode inductance of a trace above a ground plane, with and without a metallic cover above the trace.

III. Relation of the PCB near field to the cavity field

In Section II we described the relation between the cavity field and common mode coupling to cables. Only the vertical current segments of a trace couple to the cavity, according to [4]. High currents on PCB traces and ICs are identified from a near field magnitude scan. The vertical currents in the scan plane

$$Is_i = \int_{A_i} J_s \mathrm{d}A = \int_{A_i} \left(\frac{\partial}{\partial x} H_y - \frac{\partial}{\partial y} H_x \right) \mathrm{d}A, \qquad (23)$$

are obtained from the measured magnetic near field values H_x and H_y. J_s is the vertical current density and A_i denotes the area of the scan plane assigned to the vertical current with the index i. Fig.8 depicts the described procedure of obtaining the vertical currents from the measured near field above a trace.

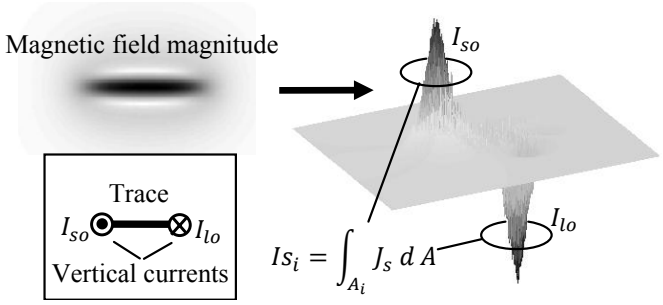

Fig. 8. Example of obtaining the vertical currents of a trace from the magnetic near field.

In Section II we obtained the cavity field from the vertical trace currents I_i weighted with d/h. According to

$$I_i = Is_i \frac{d_s}{d} \qquad \Rightarrow \qquad I_i \frac{d}{h} = Is_i \frac{d_s}{h}, \qquad (24)$$

where d_s denotes the height of the scanning plane above the parallel ground plane, the currents Is_i from (23) with the weighting factor

$$K_{couple} = d_s/h, \qquad (25)$$

excite the same cavity field. Thus, the cavity field and the common mode coupling to cables are obtained from a scan measurement, without knowledge of d and I_i. Equation (23) reveals that not the field density values, but their derivatives are significant for the coupling to the cavity. The cavity field can be obtained from the scanned field up to high cavity modes, when the field scan provides magnitude and phase information. Phase information can either be obtained with a double probe time domain scanner [10], or by the method of [11], which obtains the phase from two magnitude scans with different scan heights above the PCB. For electrically short traces with $l_t < 10\lambda$, the phase relation between the vertical trace currents is nearly 180^{o} and thus, the vertical currents can be obtained from introducing only the magnitudes of the scanned magnetic fields to (23). For this purpose, current flow lines and their associated vertical current positions are identified from the near field magnitude plot. Thus, electrically short traces or ICs can be classified regarding their common mode coupling from magnetic field magnitude scans. IC EMC testing according to IEC61967 requires a costly test board and the coupling from the test board to the septum cannot be distinguished from the IC coupling. The proposed method avoids these disadvantages.

IV. Conclusions

The common mode coupling to cables of a PCB inside a parallel plane cavity can be obtained from the field which is coupled from the PCB to the cavity. This cavity field can be obtained from the near field above the PCB. For electrically short PCB traces and for ICs, the common mode coupling can be obtained just from a magnetic near field magnitude information. The design expression (22) for the common mode inductance provides an efficient first order information about the common mode coupling of PCB traces inside a cavity.

Acknowledgment

This work was supported by the Austrian Research Promotion Agency (FFG) in the Parachute program.

References

[1] D. M. Hockanson, J. L. Drewniak, T. H. Hubing, T. P. V. Doren, F. Sha, and M. J. Wilhelm, "Investigation of fundamental EMI source mechanisms driving common-mode radiation from printed circuit boards with attached cables," in *IEEE Transactions on Electromagnetic Compatibility*, vol. 38, no. 4, November 1996, pp. 557–566.

[2] B. Deutschmann, H. Pitsch, and G. Langer, "Near field measurements to predict the electromagntic emission from integrated circuits," in *Proceedings of the 5th International Workshop on Electromagnetic Compatibility of Integrated Circuits*, November 2005, pp. 27–32.

[3] C. Labussiere, C. Lochot, and A. Boyer, "Characterization of the radiation from a 16-bit microcontroller by using miniature near-field probes," in *Proceedings of the 5th International Workshop on Electromagnetic Compatibility of Integrated Circuits*, November 2005, pp. 33–38.

[4] C. Poschalko and S. Selberherr, "Cavity model for the slot radiation of an enclosure excited by printed circuit board traces with different loads," in *IEEE Transactions on Electromagnetic Compatibility*, vol. 51, no. 1, February 2009, pp. 18–24.

[5] D. M. Hockanson, J. L. Drewniak, T. H. Hubing, T. P. V. Doren, C.-W. L. Fei Sha, and L. Rubin, "Quantifying EMI resulting from finite-impedance reference planes," *IEEE Transactions on Electromagnetic Compatibility*, vol. 39, no. 4, pp. 286–297, November 1997.

[6] M. Leone, "Design expressions for the trace-to-edge common-mode inductance of a printed circuit board," in *IEEE Transactions on Electromagnetic Compatibility*, vol. 43, no. 4, November 2001, pp. 667–671.

[7] S. Deng, T. Hubing, and D. G. Beetner, "Characterizing the electric field coupling from IC heatsink structures to external cables using TEM cell measurements," in *IEEE Transactions on Electromagnetic Compatibility*, vol. 49, no. 4, November 2007, pp. 785–791.

[8] S. Deng, T. H. Hubing, and D. G. Beetner, "Using TEM cell measurements to estimate the maximum radiation from PCBs with cables due to magnetic field coupling," in *IEEE Transactions on Electromagnetic Compatibility*, vol. 50, no. 2, May 2008, pp. 419–423.

[9] C. Wang, J. Mao, G. Selli, S. Luan, L. Zhang, J. Fan, D. J. Pommerenke, R. E. DuBroff, and J. L. Drewniak, "An efficient approach for power delivery network design with closed-form expressions for parasitic interconnect inductances," in *IEEE Transactions on Advanced Packaging*, vol. 29, no. 2, May 2006, pp. 320–334.

[10] T. Stadtler, L. Eifler, and J. L. t. Haseborg, "Double probe near field scanner, a new device for measurements in time domain," in *IEEE Symposium on Electromagnetic Compatibility*, vol. 1, August 2006, pp. 86–90.

[11] P. Kralicek, *Makromodellierung des Strahlungsverhaltens von Subsystemen zur Systemanalyse*. Dissertation, Institut für Grundlagen der Elektrotechnik und Messtechnik der Universität Hannover, November 2006, ch. Bestimmung der Multipolmomente aus den Betragsdaten, pp. 47–55.